AGU100 ADVANCING EARTH AND SPACE SCIENCE

Geophysical Research Letters

RESEARCH LETTER
10.1029/2019GL086930

Key Points:
- North Atlantic tropical cyclone frequency decreases and median intensity increases in future CAM5 climate change projection simulations
- Due to less tropical cyclone landfalls in the United States, tropical cyclone precipitation over land decreases in CAM5 in the future
- Higher precipitation rates in future climate projections increase the amount of precipitation produced per hour of tropical cyclone impact

Supporting Information:
- Supporting Information S1

Correspondence to:
A. M. Stansfield,
alyssa.stansfield@stonybrook.edu

Citation:
Stansfield, A. M., Reed, K. A., & Zarzycki, C. M. (2020). Changes in precipitation from North Atlantic tropical cyclones under RCP scenarios in the variable-resolution community atmosphere model. *Geophysical Research Letters*, *47*, e2019GL086930. https://doi.org/10.1029/2019GL086930

Received 2 JAN 2020
Accepted 19 APR 2020
Accepted article online 30 MAY 2020

Changes in Precipitation From North Atlantic Tropical Cyclones Under RCP Scenarios in the Variable-Resolution Community Atmosphere Model

Alyssa M. Stansfield[1], Kevin A. Reed[2], and Colin M. Zarzycki[2]

[1]School of Marine and Atmospheric Sciences, Stony Brook University, Stony Brook, NY, USA, [2]Department of Meteorology and Atmospheric Science, Pennsylvania State University, University Park, PA, USA

Abstract Decreasing climate models' grid spacing improves the representation of tropical cyclones at decadal time scales. In this study, a variable-resolution (VR) version of the Community Atmosphere Model 5 (CAM5-VR) is utilized to study North Atlantic tropical cyclone climatology in ensemble historical climate simulations and under two Representative Concentration Pathway (RCP) projections (RCP4.5 and RCP8.5). Basin-wide tropical cyclone counts decrease in the RCP simulations, although landfalling storm counts do not show as straightforward of a pattern, especially when focusing on regional changes. Lifetime maximum intensity metrics suggest that tropical cyclones increase in strength in the RCP ensembles. However, despite increases in tropical cyclone-related precipitation rates and the amount of precipitation produced per storm with warming, the annual average Rx5day from tropical cyclones over the eastern United States decreases due to less landfalling storms. This work is part of a continued effort to quantify how tropical cyclone-induced hazards may change in future climates.

Plain Language Summary Landfalling tropical cyclones create dangerous conditions for residents of the eastern United States through heavy rainfall, strong winds, and storm surge. This work utilizes a global climate model to estimate how these hazards from such storms might change in the future by studying changes in the tropical cyclones' intensities, sizes, and rainfall accumulations. In these climate model simulations, the number of tropical cyclones in the North Atlantic decreases and so does the number of tropical cyclones that make landfall in the United States in the future climate projections. The average intensities of these storms increase. The rainfall intensities within the tropical cyclones also increase in the future climate projections, so that the amount of rainfall produced per storm increases. Based on our simulations, although the number of tropical cyclones that make landfall in the United States will decrease in the future, the amount of precipitation that each landfalling storm produces will increase.

1. Introduction

The confidence in the credibility of future tropical cyclone (TC) projections has been increasing as the resolution of climate models increases in step with advancements in computational efficiency. High-resolution (≈50 km grid spacing and finer) global climate models can simulate a TC climatology that is similar to observations for TC counts, track patterns, and in some cases maximum lifetime intensities (e.g., Bacmeister et al., 2014; Camargo & Wing, 2016; Chauvin et al., 2019; Kim et al., 2014; Murakami et al., 2015; Roberts et al., 2020; Scoccimarro et al., 2020; Shaevitz et al., 2014; Wehner et al., 2014, 2017). Despite the presence of some systematic biases in the models, it is still worthwhile to explore changes in model TCs under estimated climate change forcings. Most studies agree that global TC counts will decrease due to climate change but that the average intensities of storms that do form will increase (e.g., Bacmeister et al., 2018; Gutmann et al., 2018; Kim et al., 2014; Knutson et al., 2015; Wehner et al., 2015); however, some studies suggest that TC counts may increase or remain about the same as the present climate, but agree with the consensus that their intensities will increase (Bhatia et al., 2018; Emanuel, 2013; Vecchi et al., 2019). How much TC intensities increase with the current rate of warming is speculated to depend on the future regional patterns of sea surface temperature (SST) changes, which are uncertain (Camargo & Wing, 2016; Murakami & Wang, 2010; Zhao & Held, 2012). Additionally, some studies suggest that average TC sizes may be increasing

due to climate change, although this may vary by ocean basin (Gutmann et al., 2018; Kim et al., 2014; Knutson et al., 2015; Sun et al., 2017; Yamada et al., 2017).

Several recent studies show that as the climate continues to warm, TCs are expected to produce more precipitation, although the projection of how much more precipitation depends on the specifics of the study. A summary of eight studies estimates a global mean increase in TC near-storm precipitation rate of about 14% per 2° of warming; however, this result is a global mean and could vary by ocean basin (Knutson et al., 2019). For the eastern United States, Wright et al. (2015) used dynamical downscaling with a high-resolution regional climate model to examine projected changes in TC precipitation in three different future climate scenarios. They generally found increased TC precipitation over the study region in the future scenario simulations, although there were some areas with decreased TC precipitation, depending on the exact scenario; however, the domain-averaged TC precipitation was greater in all the climate change projection simulations than the present-day control simulation. Similarly, Liu et al. (2018) examined TC precipitation over the eastern United States but using a global climate model under the Representative Concentration Pathway (RCP4.5) scenario. They found decreasing landfalling TC frequency in the southern United States and variable changes in TC precipitation, both increases and decreases. They related this to the competing effects of decreasing TC landfalls and increasing precipitation rates. For the Northeast, they found a slight increase in TC track density and an increase in TC precipitation near the coasts but a decrease more inland.

This study compares characteristics of North Atlantic TCs in a historical climate simulation and two climate change projection simulations. Specifically, we focus on how TC counts, both basin-wide and landfalling in the United States, and TC-related extreme precipitation might change under the influence of climate change. Changes in TC intensities and outer sizes are also discussed. Section 2 describes the climate model and analysis methodology. Section 3 presents the results of the study, and section 4 further discusses the results and provides conclusions.

2. Data and Methods

2.1. Description of Model Simulations

The numerical model used for this study is the Community Atmosphere Model version 5 (CAM5) (Neale & Coauthors, 2012), the atmospheric component of the Community Earth System Model (CESM). The spectral element dynamical core (Dennis et al., 2012; Taylor, 2011; Taylor et al., 1997) is used with the default CAM5 physical parameterization package (Neale & Coauthors, 2012), including the Zhang-McFarlane deep convection scheme (Zhang & McFarlane, 1995) and Park and Bretherton shallow convection scheme (Park & Bretherton, 2009). Specifically, the variable-resolution (VR) version of CAM5 (Zarzycki et al., 2014) is run, with grid spacing of about 111 km over most of the global domain and grid spacing of about 28 km over the North Atlantic basin. VR is advantageous because errors associated with boundary conditions are reduced and the simulations are much less computationally expensive than global high-resolution runs (Wehner et al., 2017; Zarzycki & Jablonowski, 2014). This particular VR setup was chosen to study the impact of climate change on TCs in the North Atlantic based on results from Stansfield et al. (2020), which concluded that a CAM5-VR version with refinement over the North Atlantic basin provided the best balance between computational efficiency and quality representation of TC climatology compared to two other VR setups with smaller or larger high-resolution domains. Based on previous studies that compared output from similar CAM5-VR configurations to global high-resolution CAM configurations (Zarzycki et al., 2014; Zarzycki & Jablonowski, 2015), it is expected that the CAM5-VR setup would produce similar regional climatology to a global high-resolution configuration, at a fraction of the computational cost.

The current day "reference" simulation (REF) was run under Atmospheric Model Intercomparison Project (AMIP) conditions with prescribed SSTs, sea ice, and greenhouse gas concentrations from 1984–2014, with 1984 discarded for spin-up. One year of spin-up time is standard for multidecadal, uncoupled CAM simulations (Wehner et al., 2014; Zarzycki & Jablonowski, 2014). Comparison of TC precipitation metrics between the REF simulation and observations is discussed in the supporting information (Text S2 and Figure S1). Two additional simulations were performed using the Representative Concentration Pathway scenarios (Van Vuuren et al., 2011) (i.e., RCP4.5 and RCP8.5) and are integrated from 2069–2100 (with 2069 discarded for spin-up). These RCP scenarios serve as potential future climate change scenarios with different rates of emissions of greenhouse gases, aerosols, and chemically active gases where RCP8.5 represents a higher emissions scenario than RCP4.5. SSTs for the RCP simulations were bias-corrected using a fully coupled

CESM run, as described in Bacmeister et al. (2018), although for this study only one projected SST pattern is used for each RCP scenario. For each of the three CAM5 configurations, three ensemble members were created by slightly varying the initial state.

2.2. TC Tracking in the Model Output

The TempestExtremes package (Ullrich & Zarzycki, 2017; Zarzycki & Ullrich, 2017) is utilized to track TCs in the model output and extract precipitation related to those TCs. Based on sea level pressure minima and warm core characteristics, candidate cyclones are identified on the native model grid and then connected together to create TC tracks. For each TC at each time step in its lifetime, radial profiles of the azimuthal wind speed are calculated from the zonal and meridional wind components at the lowest model level (≈64 m above the surface) following the process described in Chavas et al. (2015). The largest radius outside of the TC's eyewall where the radial wind profile exceeds 8 m/s ($r8$) is identified and used to define the outer size of the TC. At each time step of each TC's lifetime, 6-hourly averaged precipitation within $r8$ is recorded as the TC-related precipitation. More details on this tracking and precipitation extraction process can be found in the supporting information, and the TempestExtreme commandline can be found in Stansfield et al. (2020).

2.3. Metrics and Diagnostics

To study overland TC track climatology beyond landfalling storm counts, TC track density is calculated. Track density is calculated as the sum of all points within each storm's $r8$ at all times during the TCs' lifetimes, multiplied by 6 to convert to hours (model variables needed for tracking are output at 6 hr increments), and divided by the number of years of model output. Track density, as defined here, provides a measure of the number of hours per year a given point is impacted by TCs. The extreme precipitation diagnostic used in this study is the annual maximum 5-day precipitation total (Rx5day). This diagnostic has been used by Sanderson and Wehner (2017) in the Fourth National Climate Assessment to compare the prediction skill of different CMIP5 models. TC-related Rx5day is calculated by summing up TC-related precipitation at each grid point for each 5-day window for each year. The maximum 5-day total is then found for each point, and that total is recorded as the Rx5day for that individual grid point for a given year. Rx5day is more applicable for TC precipitation analysis than a single day precipitation maximum because TCs often produce precipitation over the same areas for multiple days. This metric analysis is completed for each year of the model simulations, and the mean Rx5day is calculated by averaging over time for each grid point. In addition, extreme precipitation is also analyzed using probability distribution functions (PDFs), which show how likely extreme precipitation rates are to occur in the different model simulations, both for overall precipitation and TC-related precipitation.

3. Results

3.1. TC Counts, Intensities, and Sizes

First, we compare TC counts, intensities, and sizes between the three simulations. For basin-wide storm counts, results are similar to previous studies of North Atlantic TCs under climate change (e.g., Bacmeister et al., 2018; Bhatia et al., 2018; Chauvin et al., 2019; Kim et al., 2014; Knutson et al., 2019; Moon et al., 2019; Wehner et al., 2018). Annual mean TC counts are lower in the RCP simulations compared to the REF (Table 1). When comparing the ensemble mean statistics, basin-wide TC counts decrease by 22% comparing REF to RCP4.5 and by 32% comparing REF to RCP8.5. Both of these differences are statistically significant at the 5% level. When focusing only on continental United States landfalling storms, the total annual mean landfalling counts still decrease in the RCP simulations, but at the regional level (using National Climate Assessment regions from USGCRP, 2017), the changes in landfalling frequency are less clear. The total annual mean landfalling TC counts decrease by about 27% comparing REF to RCP4.5 and by about 32% comparing REF to RCP8.5. The only United States region where projected landfalls show a consistent decrease is the Southern Plains. For the Southeast, annual mean landfalls decrease comparing REF to RCP4.5 but then are slightly lower for RCP4.5 than for RCP8.5, although the RCP8.5 value is still 24% smaller than the REF value. In the Northeast, annual mean landfalls are larger in RCP4.5 than REF but the RCP8.5 count is lower than both REF and RCP4.5 (Table 1). The higher variability between scenarios in regional landfalling TC counts than in basin-wide TC counts may reflect uncertainties in projections of changes in regional SST patterns (Camargo & Wing, 2016; Zhao & Held, 2012), uncertainties in the variability of

Table 1
Annual Mean North Atlantic TC Counts [Number per Year], Annual Mean Ensemble Mean Continental United States Landfalling TC Counts Separated by NCA Region [Number per Year], Medians and 95th Percentiles of Lifetime Maximum Near-Surface Wind Speed Distributions [m/s], medians and 5th percentiles of lifetime minimum minimum sea level pressure distributions [hPa], and medians and 95th percentiles of r8 distributions [km]

Metric	REF	RCP4.5	RCP8.5
	Total North Atlantic TC Count Per Year		
Ensemble mean	12.5 [12.2–12.7]	9.7*[9.5–10.0]	8.5*[7.5–9.6]
	Landfalling TC count per year		
Southeast	1.47 [1.33–1.60]	1.05 [0.97–1.19]	1.11 [0.94–1.19]
Northeast	0.16 [0.10–0.23]	0.22 [0.16–0.26]	0.13 [0.03–1.19]
Southern Plains	0.36 [0.13–0.6]	0.18 [0.10–0.23]	0.11* [0.03–1.19]
Total	1.98 [1.73–2.16]	1.45 [1.45–1.45]	1.34 [1.13–1.58]
	Lifetime maximum intensity—wind speed		
Median	28.9 [28.8–29.2]	29.0 [28.5–29.6]	29.5* [28.4–30.7]
95th percentile	63.9 [62.6–65.2]	62.1 [58.4–65.1]	59.4 [56.9–60.2]
	Lifetime maximum intensity—minimum sea level pressure		
Median	988.3 [987.2–989.1]	988.4 [987.1–990.2]	986.3 [983.6–987.9]
5th percentile	925.0 [924.8–926.0]	926.0 [919.0–928.5]	933.4 [930.9–934.4]
	Outer storm size		
Median	457.9 [471.8–458.0]	513.4* [485.6–527.3]	541.1* [513.4–555.0]
95th percentile	1,248.8 [1,221.0–1,276.5]	1,443.0 [1,429.1–1,456.9]	1,456.9 [1,443.0–1,481.1]

Note. For all metrics, only TCs that reach a lifetime maximum near-surface wind speed of 17 m/s are counted. Mean and median values for RCP4.5 and RCP8.5 marked with an asterisk are significantly different from the REF value at the 5% level. Significance was tested for the TC count ensemble means using the test for the difference between two Poisson rates (Mathews, 2010) and for the medians of the intensity and size distributions using K-S tests. To demonstrate the variability between the ensemble members, value ranges within the brackets represent the highest and lowest values of that variable among the three ensemble members.

atmospheric aerosols that can impact regional TC genesis (Reed et al., 2019; Sobel et al., 2019), and/or natural internal variability of the climate system (Kossin et al., 2010; Larson et al., 2005; Xie et al., 2002).

To examine TC intensities, distributions of lifetime maximum wind speed and minimum sea level pressure are created for each simulation (Figure 1). The medians of the distributions suggest a slight shift toward more intense storms in the RCP simulations, but the 95th percentiles (5th percentiles for minimum sea level pressure) show a slight weakening in intensity in the RCP simulations compared to REF (Table 1). The shift of the medians toward more intense TCs is consistent with direct multidecadal simulations of TCs in warmer climates (e.g., Bacmeister et al., 2018; Gutmann et al., 2018; Kim et al., 2014; Knutson et al., 2015; Vecchi et al., 2019; Wehner et al., 2015) as well as with theoretical arguments based on increases in environmental potential intensity (e.g., Emanuel, 2004; Sobel et al., 2016; Wang et al., 2014; Yu et al., 2010). This result could be influenced by the decrease in Categories 4 and 5 storms in the RCP4.5 and RCP8.5 scenarios compared to REF (not shown), which is related to the decrease in the overall TC counts (Table 1). While maximum potential intensity (Bister & Emanuel, 2002) increases over most of the tropical North Atlantic in the RCP simulations compared to REF, the genesis potential index (Emanuel, 2010) decreases (see Figure S2), which is consistent with the decrease in TC counts in the RCP simulations. Also, it is important to note that this distribution tail intensity analysis is limited by the resolution of the numerical model, and a model with ≈28 km horizontal grid spacing is likely not appropriate for making conclusions about changes in Categories 4 and 5 TCs in future warming scenarios (Davis, 2018). Based on a two-sample Kolmogorov-Smirnov test, the only intensity distributions that are significantly different at the 5% level are the REF and RCP8.5 maximum wind speed distributions. Distributions of outer storm sizes, taken to be the radius of the 8-m/s wind, suggest that TCs increase in size in warmer climates. The distribution median increases by 12% comparing REF to RCP4.5 and by about 18% comparing REF to RCP8.5, with the 95th percentile events showing a similar change (Table 1). All of the outer size distributions are significantly different at the 5% level.

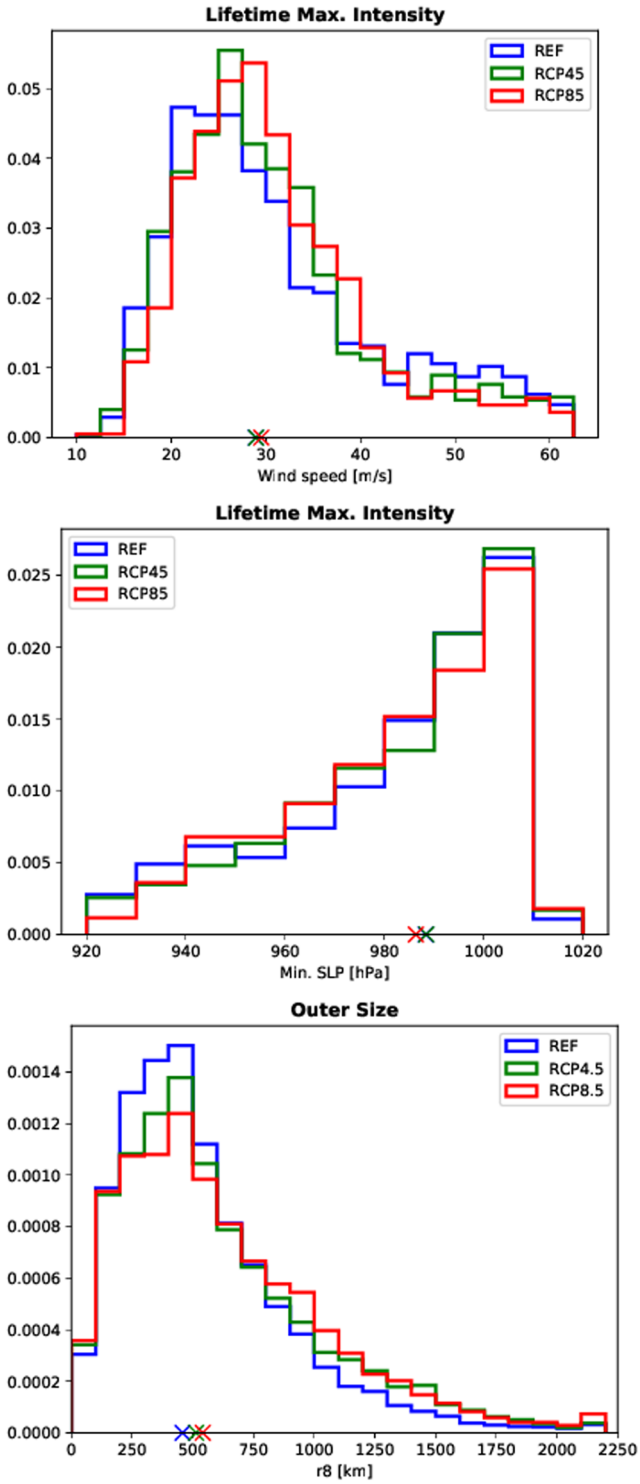

Figure 1. Histograms of lifetime maximum intensity measured by wind speed [m/s] (top), by minimum sea level pressure [hPa] (middle), and TC outer size measured by the radius of the 8-m/s wind [km] (bottom). The X's on the *x* axis mark the medians of the distributions. Bin sizes are 2.5 m/s for wind speed, 10 hPa for minimum sea level pressure, and 100 km for outer size. The histograms are normalized such that the integral over the range is 1.

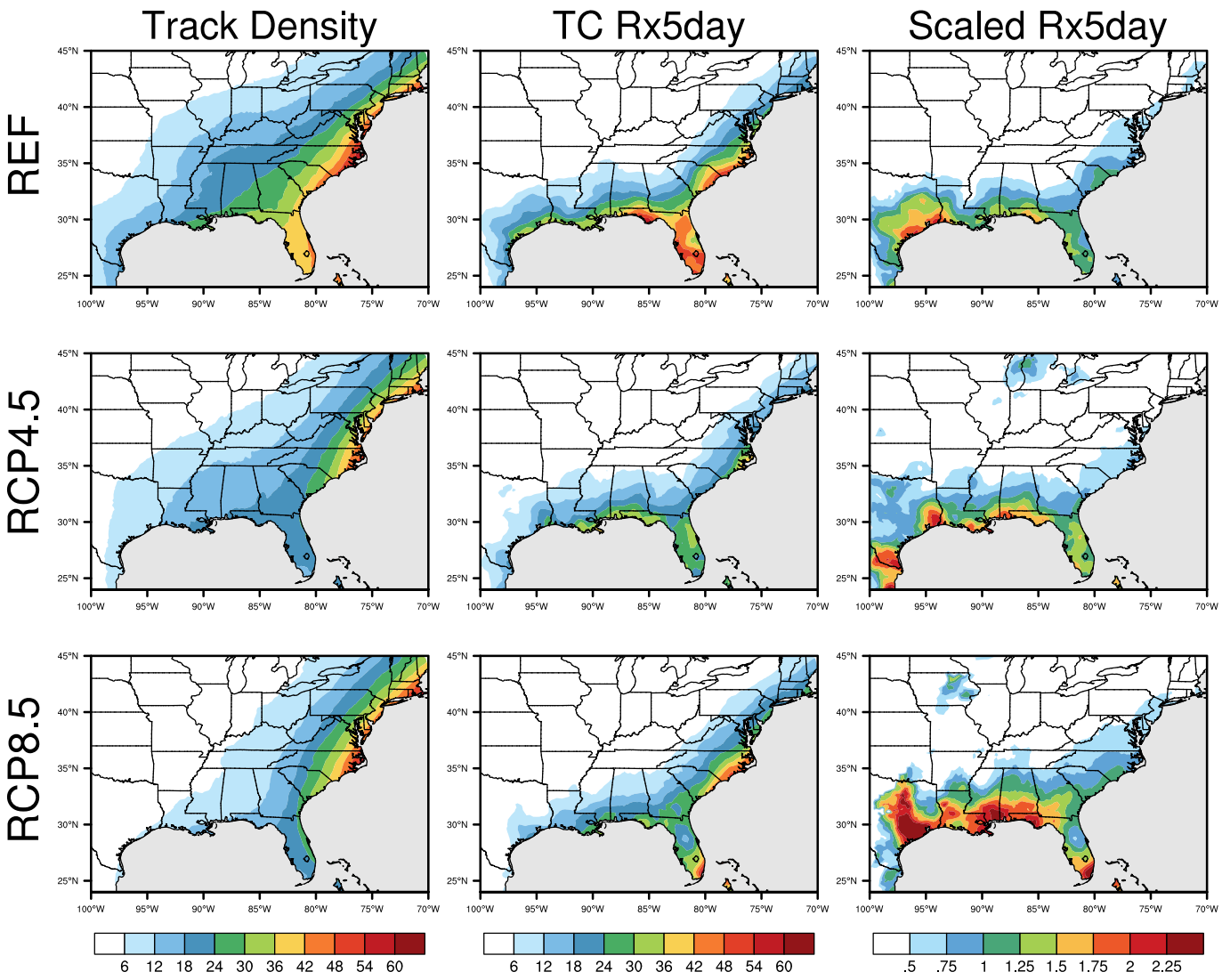

Figure 2. Annual mean TC track density [hours of TC impact per year] (left column), annual mean TC-related Rx5day [mm/yr] (middle column), and annual mean TC-related Rx5day divided by annual mean TC track density [mm/hr of impact] (right column) for REF (top row), RCP4.5 (middle row), and RCP8.5 (bottom row). For right column, only points where the track density is greater than 1.5 hr of impact per year are included.

3.2. TC Precipitation

3.2.1. Precipitation Over the Eastern United States

The annual mean precipitation produced by TCs over the eastern United States depends on how many TCs make landfall per year and where they make landfall, as well as the amount of precipitation that each TC creates (Barlow, 2011; Emanuel, 2017; Kunkel et al., 2010; Liu et al., 2018; Scoccimarro et al., 2014; Stansfield et al., 2020; Wright et al., 2015). The left column of Figure 2 shows the annual mean track density for REF, RCP4.5, and RCP8.5. Along the Atlantic coast north of South Carolina, the track density appears about the same in all simulations, except for a subtle increase over Massachusetts, Connecticut, and New Hampshire in RCP8.5 compared to REF. The track density is lower over most of the Southeast and Gulf Coast for both RCP simulations when compared to the REF simulation, which agrees with the decrease in the landfalling TC counts per year in the Southeast (Table 1). One of the clearest differences between REF and both RCP simulations is the decrease in track density over Florida, which goes from a track density of around 36–42 hr of TC impact per year in REF to about 18–24 hr in RCP4.5 and RCP8.5. These results are consistent with Liu et al. (2017), who also found decreasing TC track density over the Gulf Coast and Florida in climate change projections using the RCP4.5 scenario, although they examined years 2056–2100 in their simulations. They also found increasing track density off the coast of the Northeast, but only for extratropical transitioning TCs.

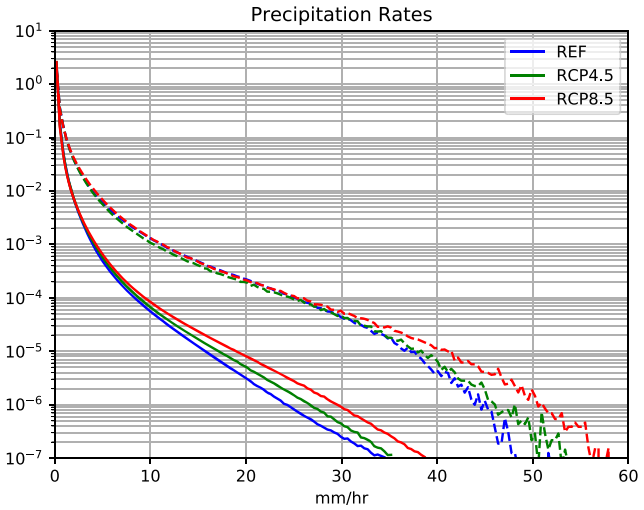

Figure 3. Probability density of all (solid lines) precipitation rates [mm/hr] and TC-related (dashed lines) precipitation rates [mm/hr] for REF, RCP4.5, and RCP8.5 for all three ensemble members combined. Only nonzero precipitation rates are included. For each PDF, the data are binned into 200 bins using a range of 0 to 70 mm/hr, resulting in bin sizes of 0.35 mm/hr. The number of values included in the all precipitation rates PDFs are $9.03e^9$ for REF, $9.29e^9$ for RCP4.5, and $9.02e^9$ for RCP8.5. The number of values included for the TC precipitation PDFs are $4.58e^7$ for REF, $3.96e^7$ for RCP4.5, and $3.71e^7$ for RCP8.5.

Although the annual mean TC track density over Florida decreases in the RCP simulations, the annual mean TC-related Rx5day does not follow the same pattern (Figure 2, middle column). Over southeast Florida, the Rx5day decreases by about 20–30 mm/yr comparing REF to RCP4.5 but then it is larger for RCP8.5 than RCP4.5. A similar pattern is also obvious over the coast of the Carolinas. In most other areas, such as most of the Gulf Coast, Florida, and Georgia, the TC-related Rx5day is lower in the RCP simulations compared to the REF. This decrease in annual mean extreme precipitation from TCs is linked to the decreasing annual mean TC track density, especially over the Gulf Coast. The same pattern of change is seen for annual mean TC-related precipitation (Figure S3, middle column). These results are similar to results described in Liu et al. (2018). Using RCP4.5 for future climate projections for years 2056–2100, they also found decreasing track density over the Southeast in the future compared to a present-day simulation. However, the changes in TC-related precipitation in their simulations were very heterogeneous in the southern United States, with some areas showing a decrease and some an increase, while results from this study indicate only decreasing TC-related Rx5day (Figure 2) and TC precipitation (Figure S3) in the RCP4.5 simulations compared to the REF.

The right column of Figure 2 shows "scaled Rx5day," which is simply the annual mean TC-related Rx5day from the middle column divided by the annual mean TC track density from the left column. This precipitation metric has units of rainfall in mm per hours of TC impact, so it quantifies an annual mean of how much extreme precipitation is produced per every hour of TC impact at each location. The annual mean scaled Rx5day is larger along most of the Gulf Coast in the RCP simulations than the REF, with the largest differences appearing between the REF and RCP8.5. The scaled Rx5day does not change much along the Atlantic Coast, except for the southern tip of Florida. Increases in this diagnostic suggest that, on average, the most extreme TC precipitation events are producing more precipitation per hour of TC lifetime, which implies that precipitation rates within these storms are increasing. This, in part, explains why certain areas, such as Southern Florida, show decreased track density in the RCP simulations compared to REF but comparable TC-related Rx5day. Despite a reduction in landfalling TCs in the RCP simulations, the TCs are capable of producing more precipitation and therefore result in TC extreme precipitation amounts that remain the same or even increase in some areas. This precipitation analysis was also completed for annual mean TC-related precipitation and showed very similar results as TC-related Rx5day (Figure S3). To see the difference plots between the model simulations for Figure 2, see Figure S4 in the supporting information.

3.2.2. Precipitation Rates

To look more closely at the extreme precipitation rates in the simulations, Figure 3 shows probability density functions for 6-hourly precipitation rates for all precipitation rates (solid lines) and for just precipitation rates within TCs (dashed lines). Note that for all distributions, only precipitation rates for model gridpoints within the high-resolution region of the VR grid are included to avoid the influence of coarser model resolution on precipitation rates. For the distributions of all precipitation rates, the lower end of the distributions look about the same up until about 5 mm/hr, when the distributions start to diverge. After that point, the probabilities of any given precipitation rate increase going from REF to RCP4.5 and from RCP4.5 to RCP8.5. The TC-related precipitation rate distributions show a similar pattern, but their distributions do not begin to diverge until around 30 mm/hr. To give an example, the probability of a 40 mm/hr precipitation rate in TCs increases by about 58% between REF and RCP4.5 and by about 75% between REF and RCP8.5. These results back up the assertion from Section 3.2.1 that more extreme precipitation rates within TCs in warmer climates increases the amount of precipitation that TCs produce per hour of impact. Additionally, these results are consistent with Wright et al. (2015) and Liu et al. (2018), which both showed increased precipitation rates in TC composite radial precipitation profiles in future climate change projection simulations.

4. Conclusions

This study utilizes a variable-resolution version of CAM5 to study the changes in North Atlantic TC climatology related to climate change, with specific focus on extreme precipitation over the eastern United States. For the historical climate simulation AMIP protocols are used, while for the future climate simulations the RCP4.5 and RCP8.5 scenarios are used. Multidecadal simulations of TCs are analyzed and compared between the climate configurations. TCs are tracked and TC-related precipitation is extracted based on the estimated sizes of the outer circulations of the storms using the TempestExtremes package (Ullrich & Zarzycki, 2017). More details on this process can be found in the supporting information. TC counts, landfalling frequency, intensities, outer sizes, and extreme precipitation are compared between the simulations to estimate the impacts of climate change on TCs in the North Atlantic.

For TC counts and intensity changes, the results agree with most previous work on North Atlantic TCs. Total basin-wide TC counts decrease in the RCP simulations compared to the historical simulation (REF) and thus total continental United States landfalling storms also decrease, with some varying results when looking at specific coastal regions. Median TC intensity metrics tend to shift toward more intense storms in the RCP scenarios, although only the REF and RCP8.5 maximum wind speed distributions are significantly different at the 5% significance level. The changes in the extreme precipitation from TCs (TC Rx5day) over the eastern United States show some regional dependence but generally decrease going from the REF simulation to the RCP scenarios (Figure 2, middle column) due to decreases in landfalling TCs (Table 1). However, results indicate that the extreme precipitation produced per hour of TC impact is larger in the RCP simulations than in the REF, especially along the Gulf Coast (Figure 2, right column). This result is further backed up by the increasing probabilities of extreme precipitation rates in TCs in the RCP simulations shown in Figure 3.

Results from this study of North Atlantic TCs suggest that in the future, less storms will make landfall in the eastern United States, but on average each storm will produce more precipitation through increased extreme precipitation rates. This result is important when considering the human impacts of climate change and is consistent with the consensus that precipitation rates, in general, are increasing with climate change in the United States (e.g., Easterling et al., 2017; Janssen et al., 2014; Kunkel et al., 1999, 2013). One uncertainty that remains, even with current-generation climate models, is the rate at which TC-related precipitation will increase with a warming climate. While some studies suggest that TC precipitation accumulation increases will exceed the rate expected by the Clausius-Clapeyron (C-C) relation (Liu et al., 2018; Patricola & Wehner, 2018; Risser & Wehner, 2017; Van Oldenborgh et al., 2017; Wehner et al., 2015; Wright et al., 2015), others expect the precipitation rates to obey to the C-C scaling but that more precipitation will be produced due to average TC intensity increases (Knutson et al., 2015; Liu et al., 2019; Reed et al., 2020; Villarini et al., 2014). Future work will involve using idealized climate model simulations to explore the rate of increase of TC precipitation with climate change.

Acknowledgments
This work was supported by Department of Energy Office of Science award number DE-SC0016605, "An Integrated Evaluation of the Simulated Hydroclimate System of the Continental US." This research used resources of the National Energy Research Scientific Computing Center (NERSC), a U.S. Department of Energy Office of Science User Facility operated under Contract DE-AC02-05CH11231. The model output used in this study is available via a shared web portal at https://portal.nersc.gov/archive/home/c/czarzyck/shared/www/.

References

Bacmeister, J. T., Reed, K. A., Hannay, C., Lawrence, P., Bates, S., Truesdale, J. E., et al. (2018). Projected changes in tropical cyclone activity under future warming scenarios using a high-resolution climate model. *Climatic Change*, *146*(3-4), 547–560. https://doi.org/10.1007/s10584-016-1750-x

Bacmeister, J. T., Wehner, M. F., Neale, R. B., Gettelman, A., Hannay, C., Lauritzen, P. H., et al. (2014). Exploratory high-resolution climate simulations using the Community Atmosphere Model (CAM). *Journal of Climate*, *27*(9), 3073–3099. https://doi.org/10.1175/JCLI-D-13-00387.1

Barlow, M. (2011). Influence of hurricane-related activity on North American extreme precipitation. *Geophysical Research Letters*, *38*, L04705. https://doi.org/10.1029/2010GL046258

Bhatia, K., Vecchi, G., Murakami, H., Underwood, S., & Kossin, J. (2018). Projected response of tropical cyclone intensity and intensification in a global climate model. *Journal of Climate*, *31*(20), 8281–8303. https://doi.org/10.1175/JCLI-D-17-0898.1

Bister, M., & Emanuel, K. A. (2002). Low frequency variability of tropical cyclone potential intensity 1. Interannual to interdecadal variability. *Journal of Geophysical Research*, *107*(D24), 4801. https://doi.org/10.1029/2001JD000776

Camargo, S. J., & Wing, A. A. (2016). Tropical cyclones in climate models. *Wiley Interdisciplinary Reviews: Climate Change*, *7*(2), 211–237. https://doi.org/10.1002/wcc.373

Chauvin, F., Pilon, R., Palany, P., & Belmadani, A. (2019). Future changes in Atlantic hurricanes with the rotated-stretched ARPEGE—Climate at very high resolution. *Climate Dynamics*, 1–26. https://doi.org/10.1007/s00382-019-05040-4

Chavas, D. R., Lin, N., & Emanuel, K. A. (2015). A model for the complete radial structure of the tropical cyclone wind field. part I: Comparison with observed structure. *Journal of Atmospheric Science*, *72*(9), 3647–3662. https://doi.org/10.1007/s00382-019-05040-4

Davis, C. A. (2018). Resolving tropical cyclone intensity in models. *Geophysical Research Letters*, *45*, 2082–2087. https://doi.org/10.1002/2017GL076966

Dennis, J. M., Edwards, J., Evans, K. J., Guba, O., Lauritzen, P. H., Mirin, A. A., et al. (2012). CAM-SE: A scalable spectral element dynamical core for the Community Atmosphere Model. *The International Journal of High Performance Computing Applications*, *26*(1), 74–89. https://doi.org/10.1177/1094342011428142

Easterling, D. R., Arnold, J. R., Knutson, T., Kunkel, K. E., LeGrande, A. N., Leung, L. R., et al. (2017). Precipitation change in the United States. In D. J., Wuebbles, D. W., Fahey, K. A., Hibbard, D. J., Dokken, B. C., Stewart, & T. K., Maycock (Eds.), *Climate science special report: Fourth national climate assessment, volume I* (pp. 207–230). Washington, DC, USA: U.S. Global Change Research Program.

Emanuel, K. A. (2004). Response of tropical cyclone activity to climate change: Theoretical basis. In R. J., Murnane, & K., Liu (Eds.), *Hurricanes and typhoons: Past, present, and future* (pp. 395–407). New York, NY: Columbia University Press.

Emanuel, K. A. (2010). Tropical cyclone activity downscaled from NOAA-CIRES reanalysis, 1908–1958. *Journal of Advances in Modeling Earth Systems*, *2*, 1. https://doi.org/10.3894/JAMES.2010.2.1

Emanuel, K. A. (2013). Downscaling CMIP5 climate models shows increased tropical cyclone activity over the 21st century. *Proceedings of the National Academy of Sciences*, *110*(30), 12,219–12,224. https://doi.org/10.1073/pnas.1301293110

Emanuel, K. A. (2017). Assessing the present and future probability of Hurricane Harvey's rainfall. *Proceedings of the National Academy of Sciences*, *114*(48), 12,681–12,684. https://doi.org/10.1073/pnas.1716222114

Gutmann, E. D., Rasmussen, R. M., Liu, C., Ikeda, K., Bruyere, C. L., Done, J. M., et al. (2018). Changes in hurricanes from a 13-yr convection-permitting pseudo-global warming simulation. *Journal of Climate*, *31*(9), 3643–3657. https://doi.org/10.1175/JCLI-D-17-0391.1

Janssen, E., Wuebbles, D. J., Kunkel, K. E., Olsen, S. C., & Goodman, A. (2014). Observational-and model-based trends and projections of extreme precipitation over the contiguous United States. *Earth's Future*, *2*, 99–113. https://doi.org/10.1002/2013EF000185

Kim, H.-S., Vecchi, G. A., Knutson, T. R., Anderson, W. G., Delworth, T. L., Rosati, A., et al. (2014). Tropical cyclone simulation and response to CO_2 doubling in the GFDL CM2. 5 high-resolution coupled climate model. *Journal of Climate*, *27*(21), 8034–8054. https://doi.org/10.1175/JCLI-D-13-00475.1

Knutson, T., Camargo, S. J., Chan, J. C. L., Emanuel, K., Ho, C.-H., Kossin, J., et al. (2019). Tropical cyclones and climate change assessment: Part II. Projected response to anthropogenic warming. *Bulletin of the American Meteorological Society*, *101*, E303–E322. https://doi.org/10.1175/BAMS-D-18-0194.1

Knutson, T. R., Sirutis, J. J., Zhao, M., Tuleya, R. E., Bender, M., Vecchi, G. A., et al. (2015). Global projections of intense tropical cyclone activity for the late twenty-first century from dynamical downscaling of CMIP5/RCP4. 5 scenarios. *Journal of Climate*, *28*(18), 7203–7224. https://doi.org/10.1175/JCLI-D-15-0129.1

Kossin, J. P., Camargo, S. J., & Sitkowski, M. (2010). Climate modulation of North Atlantic hurricane tracks. *Journal of Climate*, *23*(11), 3057–3076. https://doi.org/10.1175/2010JCLI3497.1

Kunkel, K. E., Andsager, K., & Easterling, D. R. (1999). Long-term trends in extreme precipitation events over the conterminous United States and Canada. *Journal of climate*, *12*(8), 2515–2527.

Kunkel, K. E., Easterling, D. R., Kristovich, D. A. R., Gleason, B., Stoecker, L., & Smith, R. (2010). Recent increases in U.S. heavy precipitation associated with tropical cyclones. *Geophysical Research Letters*, *37*, L24706. https://doi.org/10.1029/2010GL045164

Kunkel, K. E., Karl, T. R., Easterling, D. R., Redmond, K., Young, J., Yin, X., & Hennon, P. (2013). Probable maximum precipitation and climate change. *Geophysical Research Letters*, *40*, 1402–1408. https://doi.org/10.1002/grl.50334

Larson, J., Zhou, Y., & Higgins, R. W. (2005). Characteristics of landfalling tropical cyclones in the United States and Mexico: Climatology and interannual variability. *Journal of Climate*, *18*(8), 1247–1262. https://doi.org/10.1175/JCLI3317.1

Liu, M., Vecchi, G. A., Smith, J. A., & Knutson, T. R. (2019). Causes of large projected increases in hurricane precipitation rates with global warming. *npj Climate and Atmospheric Science*, *2*(1), 1–5. https://doi.org/10.1038/s41612-019-0095-3

Liu, M., Vecchi, G. A., Smith, J. A., & Murakami, H. (2017). The present-day simulation and twenty-first-century projection of the climatology of extratropical transition in the North Atlantic. *Journal of Climate*, *30*(8), 2739–2756. https://doi.org/10.1175/JCLI-D-16-0352.1

Liu, M., Vecchi, G. A., Smith, J. A., & Murakami, H. (2018). Projection of landfalling–tropical cyclone rainfall in the Eastern United States under anthropogenic warming. *Journal of Climate*, *31*(18), 7269–7286. https://doi.org/10.1175/JCLI-D-17-0747.1

Mathews, P. (2010). *Sample size calculations: Practical methods for engineers and scientists*. Painesville, OH: Mathews Malnar and Bailey.

Moon, I.-J., Kim, S.-H., & Chan, J. C. L. (2019). Climate change and tropical cyclone trend. *Nature*, *570*(7759), E3–E5. https://doi.org/10.1038/s41586-019-1222-3

Murakami, H., Vecchi, G. A., Underwood, S., Delworth, T. L., Wittenberg, A. T., Anderson, W. G., et al. (2015). Simulation and prediction of category 4 and 5 hurricanes in the high-resolution GFDL HiFLOR coupled climate model. *Journal of Climate*, *28*(23), 9058–9079. https://doi.org/10.1175/JCLI-D-15-0216.1

Murakami, H., & Wang, B. (2010). Future change of North Atlantic tropical cyclone tracks: Projection by a 20-km-mesh global atmospheric model. *Journal of Climate*, *23*(10), 2699–2721. https://doi.org/10.1175/2010JCLI3338.1

Neale, R. B., & Coauthors (2012). Description of the NCAR community atmosphere model (CAM5.0) (*NCAR/TN-486+STR*): Natl. Cent. for Atmos. Res, Boulder, Colo.

Park, S., & Bretherton, C. S. (2009). The University of Washington shallow convection and moist turbulence schemes and their impact on climate simulations with the Community Atmosphere Model. *Journal of Climate*, *22*(12), 3449–3469.

Patricola, C. M., & Wehner, M. F. (2018). Anthropogenic influences on major tropical cyclone events. *Nature*, *563*(7731), 339.

Reed, K. A., Bacmeister, J. T., Huff, J. J. A., Wu, X., Bates, S. C., & Rosenbloom, N. A. (2019). Exploring the impact of dust on North Atlantic hurricanes in a high-resolution climate model. *Geophysical Research Letters*, *46*, 1105–1112. https://doi.org/10.1029/2018GL080642

Reed, K. A., Stansfield, A. M., Wehner, M. F., & Zarzycki, C. M. (2020). Forecasted attribution of the human influence on Hurricane Florence. *Science Advances*, *6*(1), eaaw9253. https://doi.org/10.1126/sciadv.aaw9253

Risser, M. D., & Wehner, M. F. (2017). Attributable human-induced changes in the likelihood and magnitude of the observed extreme precipitation during Hurricane Harvey. *Geophysical Research Letters*, *44*, 12,457–12,464. https://doi.org/10.1002/2017GL075888

Roberts, M. J., Camp, J., Seddon, J., Vidale, P. L., Hodges, K., Vanniere, B., et al. (2020). Impact of model resolution on tropical cyclone simulation using the Highres MIP-PRIMAVERA multi-model ensemble. *Journal of Climate*, *33*, 2557–2583. https://doi.org/10.1175/JCLI-D-19-0639.1

Sanderson, B. M., & Wehner, M. F. (2017). Model weighting strategy. In D. J., Wuebbles, D. W., Fahey, K. A., Hibbard, D. J. B. C. S., Dokken, & T. K., Maycock Guide to this Report. (Eds.), *Climate science special report: Fourth national climate assessment: Volume I* (pp. 436–442). U.S. Global Change Research Program.

Scoccimarro, E., Gualdi, S., Bellucci, A., Peano, D., Cherchi, A., Vecchi, G. A., & Navarra, A. (2020). The typhoon-induced drying of the Maritime Continent. *Proceedings of the Natational Academy of Sciences (USA)*.

Scoccimarro, E., Gualdi, S., Villarini, G., Vecchi, G. A., Zhao, M., Walsh, K., & Navarra, A. (2014). Intense precipitation events associated with landfalling tropical cyclones in response to a warmer climate and increased CO_2. *Journal of Climate*, *27*(12), 4642–4654. https://doi.org/10.1175/JCLI-D-14-00065.1

Shaevitz, D. A., Camargo, S. J., Sobel, A. H., Jonas, J. A., Kim, D., Kumar, A., et al. (2014). Characteristics of tropical cyclones in high-resolution models in the present climate. *Journal of Advances in Modeling Earth Systems*, *6*, 1154–1172. https://doi.org/10.1002/2014MS000372

Sobel, A. H., Camargo, S. J., Hall, T. M., Lee, C.-Y., Tippett, M. K., & Wing, A. A. (2016). Human influence on tropical cyclone intensity. *Science*, *353*(6296), 242–246. https://doi.org/10.1126/science.aaf6574

Sobel, A. H., Camargo, S. J., Previdi, M., & Emanuel, K. A. (2019). Aerosols vs. greenhouse gas effects on tropical cyclone potential intensity. *Bulletin of the American Meteorological Society*, *99*, 1517–1519.

Stansfield, A. M., Reed, K. A., Zarzycki, C. M., Ullrich, P. A., & Chavas, D. R. (2020). Assessing tropical cyclones' contribution to precipitation over the Eastern United States and sensitivity to the variable-resolution domain extent. *Journal of Hydrometeorology*. https://doi.org/10.1175/JHM-D-19-0240.1

Sun, Y., Zhong, Z., Li, T., Yi, L., Hu, Y., Wan, H., et al. (2017). Impact of ocean warming on tropical cyclone size and its destructiveness. *Scientific Reports*, *7*(1), 1–10. https://doi.org/10.1038/s41598-017-08533-6

Taylor, M. A. (2011). Conservation of mass and energy for the moist atmospheric primitive equations on unstructured grids. In *Numerical techniques for global atmospheric models* (pp. 357–380). Berlin, Heidelberg: Springer.

Taylor, M., Tribbia, J., & Iskandarani, M. (1997). The spectral element method for the shallow water equations on the sphere. *Journal of Computational Physics*, *130*(1), 92–108. https://doi.org/10.1006/jcph.1996.5554

USGCRP (2017). Guide to this Report. In D. J., Wuebbles, D. W., Fahey, K. A., Hibbard, D. D., J., B. C., Stewart, & T. K., Maycock (Eds.), *Climate science special report: Fourth national climate assessment, volume I*. Washington, DC, USA: U.S. Global Change Research Program. https://doi.org/10.7930/J0J964J6

Ullrich, P. A., & Zarzycki, C. M. (2017). TempestExtremes: A framework for scale scale-insensitive pointwise feature tracking on unstructured grids. *Geoscientific Model Development*, *10*, 1069–1090. https://doi.org/10.5194/gmd-10-1069-2017

Van Oldenborgh, G. J., Van Der Wiel, K., Sebastian, A., Singh, R., Arrighi, J., Otto, F., et al. (2017). Attribution of extreme rainfall from Hurricane Harvey, August 2017. *Environmental Research Letters*, *12*(12), 124009. https://doi.org/10.1088/1748-9326/aa9ef2

Van Vuuren, D. P., Edmonds, J., Kainuma, M., Riahi, K., Thomson, A., Hibbard, K., et al. (2011). The representative concentration pathways: An overview. *Climatic Change*, *109*(1-2), 5. https://doi.org/10.1007/s10584-011-0148-z

Vecchi, G. A., Delworth, T. L., Murakami, H., Underwood, S. D., Wittenberg, A. T., Zeng, F., et al. (2019). Tropical cyclone sensitivities to CO_2 doubling: Roles of atmospheric resolution, synoptic variability and background climate changes. *Climate Dynamics*, *53*(9-10), 5999–6033. https://doi.org/10.1007/s00382-019-04913-y

Villarini, G., Lavers, D. A., Scoccimarro, E., Zhao, M., Wehner, M. F., Vecchi, G. A., et al. (2014). Sensitivity of tropical cyclone rainfall to idealized global-scale forcings. *Journal of Climate*, *27*(12), 4622–4641. https://doi.org/10.1175/JCLI-D-13-00780.1

Wang, S., Camargo, S. J., Sobel, A. H., & Polvani, L. M. (2014). Impact of the tropopause temperature on the intensity of tropical cyclones: An idealized study using a mesoscale model. *Journal of the Atmospheric Sciences*, *71*(11), 4333–4348. https://doi.org/10.1175/JAS-D-14-0029.1

Wehner, M. F., Prabhat, Reed, K. A., Stone, D., Collins, W. D., & Bacmeister, J. (2015). Resolution dependence of future tropical cyclone projections of CAM5.1 in the U.S. CLIVAR hurricane working group idealized configurations. *Journal of Climate*, *28*(10), 3905–3925. https://doi.org/10.1175/JCLI-D-14-00311.1

Wehner, M. F., Reed, K. A., Li, F., Bacmeister, J., Chen, C.-T., Paciorek, C., et al. (2014). The effect of horizontal resolution on simulation quality in the Community Atmospheric Model, CAM5.1. *Journal of Advances in Modeling Earth Systems*, *6*, 980–997. https://doi.org/10.1002/2013MS000276

Wehner, M. F., Reed, K. A., Loring, B., Stone, D., & Krishnan, H. (2018). Changes in tropical cyclones under stabilized 1.5 and 2.0°C global warming scenarios as simulated by the Community Atmospheric Model under the HAPPI protocols. *Earth System Dynamics*, *9*(1), 187–195. https://doi.org/10.5194/esd-9-187-2018

Wehner, M. F., Reed, K. A., & Zarzycki, C. M. (2017). High-resolution multi-decadal simulation of tropical cyclones. In J. M., Collins, & K., Walsh (Eds.), *Hurricanes and climate change* (pp. 187–211). New York, NY: Springer. https://doi.org/10.1007/978-3-319-47594-3_8

Wright, D. B., Knutson, T. R., & Smith, J. A. (2015). Regional climate model projections of rainfall from US landfalling tropical cyclones. *Climate Dynamics*, *45*(11-12), 3365–3379. https://doi.org/10.1007/s00382-015-2544-y

Xie, L., Pietrafesa, L. J., & Wu, K. (2002). Interannual and decadal variability of landfalling tropical cyclones in the southeast coastal states of the United States. *Advances in Atmospheric Sciences*, *19*(4), 677–686.

Yamada, Y., Satoh, M., Sugi, M., Kodama, C., Noda, A. T., Nakano, M., & Nasuno, T. (2017). Response of tropical cyclone activity and structure to global warming in a high-resolution global nonhydrostatic model. *Journal of Climate*, *30*(23), 9703–9724. https://doi.org/10.1175/JCLI-D-17-0068.1

Yu, J., Wang, Y., & Hamilton, K. (2010). Response of tropical cyclone potential intensity to a global warming scenario in the IPCC AR4 CGCMs. *Journal of Climate*, *23*(6), 1354–1373. https://doi.org/10.1175/2009JCLI2843.1

Zarzycki, C. M., & Jablonowski, C. (2014). A multidecadal simulation of Atlantic tropical cyclones using a variable-resolution global atmospheric general circulation model. *Journal of Advances in Modeling Earth Systems*, *6*, 805–828. https://doi.org/10.1175/2009JCLI2843.1

Zarzycki, C. M., & Jablonowski, C. (2015). Experimental tropical cyclone forecasts using a variable-resolution global model. *Monthly Weather Reviews*, *143*(10), 4012–4037. https://doi.org/10.1175/MWR-D-15-0159.1

Zarzycki, C. M., Levy, M. N., Jablonowski, C., Overfelt, J. R., Taylor, M. A., & Ullrich, P. A. (2014). Aquaplanet experiments using CAM's variable-resolution dynamical core. *Journal of Climate*, *27*(14), 5481–5503.

Zarzycki, C. M., & Ullrich, P. A. (2017). Assessing sensitivities in algorithmic detection of tropical cyclones in climate data. *Geophysical Research Letters*, *44*(2), 1141–1149. https://doi.org/10.1002/2016GL071606

Zhang, G. J., & McFarlane, N. A. (1995). Sensitivity of climate simulations to the parameterization of cumulus convection in the Canadian Climate Centre general circulation model. *Atmosphere-Ocean*, *33*, 407–446. https://doi.org/10.1080/07055900.1995.9649539

Zhao, M., & Held, I. M. (2012). TC-permitting GCM simulations of hurricane frequency response to sea surface temperature anomalies projected for the late-twenty-first century. *Journal of Climate*, *25*(8), 2995–3009. https://doi.org/10.1175/JCLI-D-11-00313.1